# Natural constraints on the gluon-quark vertex

Daniele Binosi, Lei Chang, Joannis Papavassiliou, Si-Xue Qin, and Craig D. Roberts

Phys. Rev. D **95**, 031501 — Published 7 February 2017

DOI: 10.1103/PhysRevD.95.031501

# Natural constraints on the gluon-quark vertex

Daniele Binosi,[1] Lei Chang,[2] Joannis Papavassiliou,[3] Si-Xue Qin,[4] and Craig D. Roberts[4]

[1] *European Centre for Theoretical Studies in Nuclear Physics and Related Areas (ECT*) and Fondazione Bruno Kessler Villa Tambosi, Strada delle Tabarelle 286, I-38123 Villazzano (TN) Italy*

[2] *School of Physics, Nankai University, Tianjin 300071, China*

[3] *Department of Theoretical Physics and IFIC, University of Valencia and CSIC, E-46100, Valencia, Spain*

[4] *Physics Division, Argonne National Laboratory, Argonne, Illinois 60439, USA*

In principle, the strong-interaction sector of the Standard Model is characterised by a unique renormalisation-group-invariant (RGI) running interaction and a unique form for the dressed–gluon-quark vertex, $\Gamma_\mu$; but, whilst much has been learnt about the former, the latter is still obscure. In order to improve this situation, we use a RGI running-interaction that reconciles top-down and bottom-up analyses of the gauge sector in quantum chromodynamics (QCD) to compute dressed-quark gap equation solutions with 1,660,000 distinct *Ansätze* for $\Gamma_\mu$. Each one of the solutions is then tested for compatibility with three physical criteria and, remarkably, we find that merely 0.55% of the solutions survive the test. Evidently, even a small selection of observables places extremely tight bounds on the domain of realistic vertex *Ansätze*. This analysis and its results should prove useful in constraining insightful contemporary studies of QCD and hadronic phenomena.

**1. Introduction**. Strongly-interacting theories can generate mass dynamically [1]. Discussions of this phenomenon of dynamical chiral symmetry breaking (DCSB) in the context of gluons dressing the quark propagator began with Refs. [2, 3] and have since continued vigorously. A natural tool for studying DCSB is the gap equation:

$$S^{-1}(k) = i\gamma\cdot k\, A(k^2) + B(k^2) \tag{1a}$$

$$= Z_2\,(i\gamma\cdot k + m^{\rm bm}) + \Sigma(k)\,, \tag{1b}$$

$$\Sigma(k) = Z_1 \int_{dq}^{\Lambda} g^2 D_{\mu\nu}(k-q)\frac{\lambda^a}{2}\gamma_\mu S(q)\Gamma^a_\nu(q,k), \tag{1c}$$

where the dressed-gluon propagator may be expressed via

$$p^2 D_{\mu\nu}(p) = \Delta(p^2) T_{\mu\nu}\,, \tag{2}$$

$T_{\mu\nu} = \delta_{\mu\nu} - p_\mu p_\nu/p^2$; $\Gamma^a_\nu = (\lambda^a/2)\Gamma_\nu$ is the quark-gluon vertex; $\int_{dq}^{\Lambda}$ indicates a Poincaré invariant regularisation of the integral, with $\Lambda$ the regularisation scale; $m^{\rm bm}$ is the current-quark bare mass and $Z_{1,2}$, respectively, the vertex and quark wave-function renormalisation constants, with $\zeta = 19\,$GeV the renormalisation point herein [4–7].

Whether or not DCSB emerges in the Standard Model is decided by the structure of the gap equation's kernel. Hence the basic question is: Just what form does that kernel take? Owing to asymptotic freedom, the answer is known on the perturbative domain [5–9], *viz.* on $\mathcal{A} = \{(k,q)\,|\,p^2 = (k-q)^2 \simeq k^2 \simeq q^2 \gtrsim 2\,{\rm GeV}^2\}$:

$$\tfrac{g^2}{4\pi} D_{\mu\nu}(p)\, Z_1\, \Gamma_\nu(q,k) \stackrel{\mathcal{A}}{=} \alpha_s(p^2)\, D^0_{\mu\nu}(p)\, Z_2^2\, \gamma_\nu\,, \tag{3}$$

where $\alpha_s(p^2)$ is QCD's running coupling. The question thus actually relates only to the infrared domain.

Much has been learnt about the infrared behaviour of the running coupling and dressed-gluon propagator [10–12]; and the current state of understanding is described in Ref. [13]. Namely, one may write:

$$Z_1 g^2 D_{\mu\nu}(p) \to Z_2\, 4\pi\, p^2 \hat{d}(p^2) D^0_{\mu\nu}(p)\,, \tag{4}$$

where $\hat{d}(p^2)$ is a renormalisation-group-invariant (RGI) interaction strength, which is expressed as follows:

$$p^2\hat{d}(p^2) = \alpha_s(\zeta^2)\Delta(p^2;\zeta^2)/[1+G(p^2;\zeta^2)]^2\,, \tag{5}$$

with $\Delta$ in Eq. (2) and $G$ defining the transverse piece of the gluon-ghost vacuum polarisation that appears in applying the pinch-technique (PT) [14, 15] to QCD's gauge sector [10, 16, 17]. The interaction in Eq. (5) has been computed [18] and may usefully be represented by [13]:

$$\hat{d}(s) \approx \frac{2\pi}{\omega^5}\varsigma^3\, {\rm e}^{-s/\omega^2} + \frac{2\pi\gamma_m\,\mathcal{F}(s)}{\ln[\tau + (1+s/\Lambda_{\rm QCD}^2)^2]}, \tag{6}$$

where $\gamma_m^{N_f=4} = 12/25$, $\Lambda_{\rm QCD} = 0.57\,$GeV (MOM scheme); $\tau = {\rm e}^2 - 1$ $\mathcal{F}(s) = \{1-\exp(-s/[4m_t^2])\}/s$, $m_t = 0.5\,$GeV; and $\varsigma = 0.55\,$GeV, $\omega = 0.6\,$GeV [4].

Eqs. (4)–(6) bridge a gap between "top-down" analyses of QCD's gauge sector and "bottom-up" studies of its matter sector and thus represent a unification of these approaches to determining QCD's RGI interaction. This advance was enabled by an appreciation of the dressed–gauge-boson–quark vertex' importance to DCSB, and vice versa, which had grown over many years, *e.g.* Refs. [19–39], combined with the ability to quantify its impact on hadron properties [31, 33, 40–42]. It brings us to a point from which a new branch of enquiries should begin; namely, how sensitive are DCSB and hadron properties to the form of the dressed gluon-quark vertex?

**2. Gluon-Quark Vertex**. The gluon-quark vertex in the SM Lagrangian is simple: $\Gamma^a_\mu = \Gamma^{a0}_\mu = (\lambda^a/2)\gamma_\mu$. It remains relatively simple on $\mathcal{A}$: interactions produce momentum-dependent logarithmic corrections, but no new structures become significant. However, Ward-Green-Takahashi (WGT) identities [35, 36, 43–46] entail that DCSB destroys that simplicity at infrared momenta [35, 36]. Then $\Gamma^a_\mu(q,k)$ has up to twelve independent terms, each linked to a different Poincaré-covariant Dirac-matrix structure. Half of them are only nonzero

in the chiral limit owing to DCSB, so they might act as amplifiers in the gap equation's kernel. Given the role DCSB plays in forming hadron observables, Nature must then place constraints on the strength of these terms.

In order to describe one way of elucidating natural constraints on the vertex, we first decompose it ($t = q + k$): $\Gamma_\nu(q,k) = \Gamma^{\rm BC}_\nu(q,k) + \Gamma^{\rm T}_\nu(q,k)$,

$$i\Gamma^{\rm BC}_\nu(q,k) = i\gamma_\nu \Sigma^{qk}_A + t_\nu [i\tfrac{1}{2}\gamma\cdot t\, \Delta^{qk}_A + \Delta^{qk}_B]\,, \tag{7a}$$

$$\Gamma^{\rm T}_\nu(q,k) = \sum_{i=1}^{8} T^i_\nu \tau^{qk}_i\,, \tag{7b}$$

where $\lambda^{qk}_1 = \Sigma^{qk}_A = [A(q^2) + A(k^2)]/2$, $\lambda^{qk}_2 = \Delta^{qk}_A$, $\lambda^{qk}_3 = \Delta^{qk}_B$, $\Delta^{qk}_F = [F(q^2) - F(k^2)]/[q^2 - k^2]$, $F = A, B$. The first term, Eq. (7a), expresses that part of the vertex which satisfies the Abelian WGT identity, appropriate to the PT RGI interaction and also a fair representation of existing lattice-QCD results [30]. The second term, Eq. (7b), defined using the basis in Eq. (12), describes all purely transverse contributions. Its particular form is unknown, despite continuing efforts using continuum and lattice methods [19–36, 38–40, 47–50]; but, motivated by a combination of perturbation theory and the transverse WGT identities, we propose an *Ansatz* [35, 51]:

$$\tau^{qk}_1 = a_1 \Delta^{qk}_B\,,\ \tau^{qk}_3 = -a_3 2\, k\cdot q\, \Delta^{qk}_A\,,\ \tau^{qk}_4 = a_4 \frac{4\Delta^{qk}_B}{t^{\rm T}\cdot t^{\rm T}}\,,$$
$$\tau^{qk}_5 = a_5 \Delta^{qk}_B\,,\ \tau^{qk}_8 = a_8 \Delta^{qk}_A\,, \tag{8}$$

with similar expressions for $\tau_{2,6,7}$, where $\{a_i, i = 1,\ldots,8\}$ are dimensionless constants whose values modulate the strength of the associated vertex term. This *Ansatz* is simple, involving only those functions appearing in the quark propagator, but general enough to enable a meaningful study of the vertex' impact on the gap equation's solution and hence the constraints that observables impose thereupon. (In using Eq. (7a) as part of the canonical gluon-quark vertex, some ghost-field effects are implictly absorbed into $\Gamma^{\rm T}_\nu$; and Eqs. (8) entail that some effects which might originate in the transverse-WGTIs' gauge-field-dependent line integrals might be expressed in the values of the parameters $\{a_i\}$.)

**3. Natural Constraints on the Vertex**. We are about to undertake a challenging task, so it is sensible to first remark that extant studies of the meson spectrum [40, 42] suggest that the $T^{2,6,7}_\nu$ terms in $\Gamma^{\rm T}_\nu$ are of lesser importance. Hence, we neglect them hereafter, setting $a_2 = a_6 = a_7 = 0$. Additionally, following some algebra it becomes evident that the gap equation's kernel does not depend separately on $a_4$, $a_5$, but, instead, only on the combination $a_{4\hat{5}} = a_4 - 3a_5$. Allowing for these simplifications, we proceeded to scan the vertex parameter space spanned by the constants $a_{1,3,4\hat{5},8}$, chosen within

$$\mathbb{V}_4 = \{(a_1, a_3, a_{4\hat{5}}, a_8) \\ |\, a_1, a_3 \in [-1,1], a_{4\hat{5}} \in [-7,5], a_8 \in [-5,1]\}\,. \tag{9}$$

As will subsequently become apparent, it is unnecessary to explore a larger subset of $\mathbb{R}^4$.

The scanning method is simple. Working in the chiral limit, we randomly generated a quadruplet $q = (a_1, a_3, a_{4\hat{5}}, a_8)$ and therewith formed the gluon-quark vertex, ${}^q\Gamma_\nu$; solved the gap equation with that vertex and the RGI interaction in Eq. (6); and categorised the solutions as acceptable if: $(i)$ they expressed DCSB of physically reasonable strength, *i.e.* $M^0 := M(0) \in (0.25, 0.45)\,$GeV, $(ii)$ the associated dressed-quark anomalous chromomagnetic moment (ACM) was negative-definite, as required in order satisfy constraints of perturbative QCD (pQCD) [33], and $(iii)$ the pion's leptonic decay constant was within 5% of its chiral-limit value, $f^0_\pi \approx 0.088\,$GeV [52].

The ACM distribution is explained in Refs. [33, 51] and may be estimated using ($\mathcal{c} = 1 - a_1/2$)

$$\kappa(\mathcal{m}) = 2\mathcal{m}\frac{[a_5 - \mathcal{c}]\delta_B + \mathcal{m}(1 - a_8)\delta_A}{\sigma_A + 2\mathcal{m}^2(a_3 - 1)\delta_A + 2\mathcal{m}\mathcal{c}\delta_B}, \tag{10}$$

where $\sigma_A = \Sigma^{\mathcal{m}\mathcal{m}}_A$, $\delta_{A,B} = \Delta^{\mathcal{m}\mathcal{m}}_{A,B}$, and $M(k^2) = B(k^2)/A(k^2) =: \mathcal{m}$, is the dressed-quark mass-function. Concerning $f_\pi$, absent a solution to the pion's Bethe-Salpeter equation, two approximating formulae exist: $f^{\rm PS}_\pi$ (Eq. (11), Ref. [53]) and $f^{\rm CR}_\pi$ (Eq. (4.5), Ref. [54]). We use the latter because it is more accurate [31], but the difference between them is understood and they are identical in the chiral limit when the necessary corrections to both are included [55].

*3.1 Case A*: $a_1 = 0 = a_3$. Owing to the known importance of $a_{5,8}$ in determining $\kappa(\mathcal{m})$ [33], we always include nonzero values for these coefficients. Therefore, we first selected 360,000 independent values of $q = (0, 0, a_{4\hat{5}}, a_8)$, solved the gap equation for each, and catalogued the solutions as described above. Only 6% of the parameter space survived the first cut. The volume fell to 3% when $(i)$ and $(ii)$ were applied together. Finally, just 0.4% of the 360,000 vertices considered could simultaneously satisfy $(i)$–$(iii)$. The paucity of such *Ansätze* is highlighted by the upper panel of Fig. 1: the sample space is actually larger than the planar area drawn. The lower panel of Fig. 1 shows that in this case the three criteria we've applied enforce $M^0 \in (0.26, 0.31)\,$GeV.

*3.2 Case B*: $a_1 = 0$. Here we generated 400,000 vertices. Proceeding as above, one obtains the domain of acceptable coefficients depicted in the upper panel of Fig. 2. The mass functions obtained in this instance are similar to those obtained in Case A, as illustrated by the lower panel of Fig. 2: the largest attainable value in solutions consistent with our criteria is $M^0 = 0.31\,$GeV. Notably, including $a_3 \neq 0$, acceptable solutions can be obtained within a larger domain of $a_8$ values: these two tensor structures mutually compensate. However, comparing the lower panels of Figs. 1 and 2, one sees that $a_3 \neq 0$ does not much affect the mass-function's $k^2$-dependence.

*3.3 Case C*: $a_3 = 0$. We selected 360,000 independent values of $q = (a_1, 0, a_{4\hat{5}}, a_8)$ and proceeded as before,

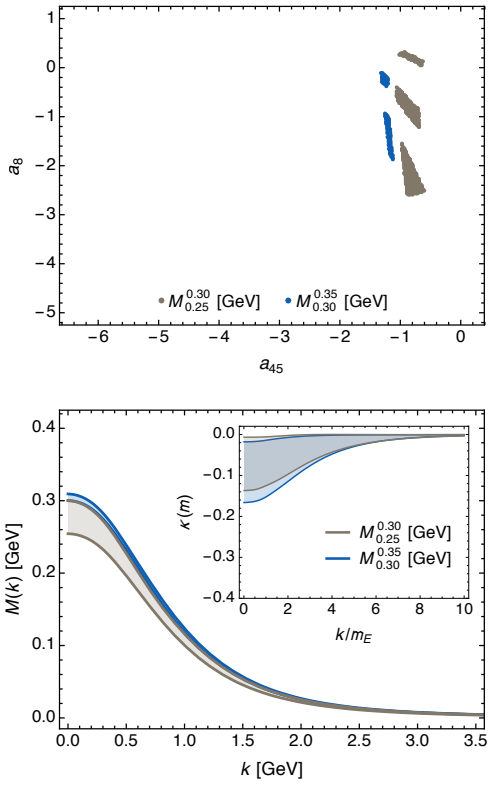


FIG. 1. Case A. *Upper panel* – Domain of coefficients $q = (0, 0, a_{4\hat{5}}, a_8)$ satisfying cuts $(i)$–$(iii)$. Bands: light (grey), $M^0 \in (0.25, 0.30)$ GeV; dark (blue), $M^0 \in (0.30, 0.35)$ GeV. *Lower panel* – Mass functions produced by the vertices identified in the upper panel lie within the like-shaded bands; and, inset, the associated anomalous chromomagnetic moment (ACM), Eq. (10). ($m_E$ is the Euclidean constituent-quark mass, *i.e.* the solution of $M(m_E) = m_E$.)

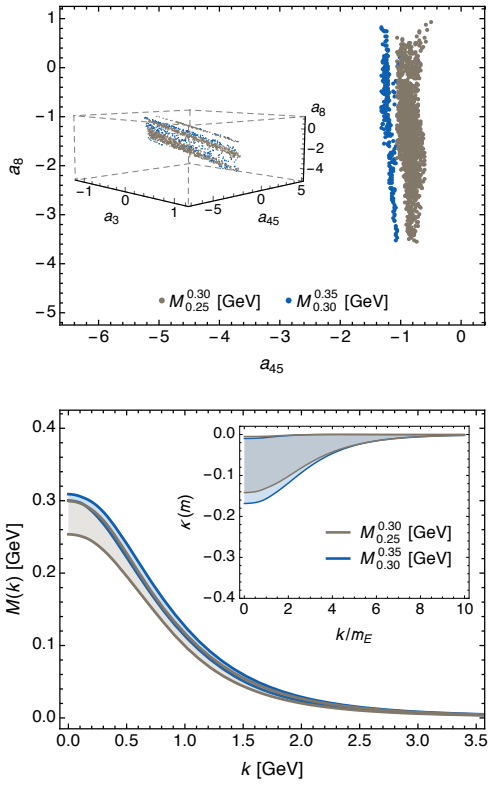


FIG. 2. Case B. *Upper panel* – Domain of coefficients $q = (0, a_3, a_{4\hat{5}}, a_8)$ satisfying cuts $(i)$–$(iii)$: the space of *Ansätze* is three-dimensional and the inset displays the volume that survives all cuts and the correlation between coefficients. *Lower panel* – Mass functions generated by the vertices identified in the upper panel lie within the like-shaded bands and produce the ACM drawn in the inserted panel. (Legend as in Fig. 1.)

with the result expressed in the upper panel of Fig. 3. Qualitatively, the outcome is similar to Case A. Successive cuts progressively restrict the space of acceptable vertex *Ansätze*, so that finally $M^0 \in (0.25, 0.36)$ GeV.

A new feature is the effect of $a_1$ on $M(k^2)$: for a fixed value of $M^0$, an increase in $a_1$ produces a steeper decline in $M(k^2)$. [We return to this point in connection with Fig. 5 below.] This might have been anticipated because, with $a_1 \neq 0$, the vertex includes a new term that depends linearly on both the magnitude and $k^2$-dependence of the dynamically generated mass function.

*3.4 Case D – all four coefficients nonzero*. We randomly selected 540,000 vertices, solved the gap equation in each case, and filtered the solutions: just 0.55% could simultaneously satisfy $(i)$–$(iii)$. The allowed *Ansätze* are identified in the upper panel of Fig. 4, with the associated mass functions depicted in the lower panel.

All features stressed already are preserved: changes in $a_3$ and $a_8$ compensate each other, but otherwise $a_3$ is only loosely constrained; $a_1$, $a_{4\hat{5}}$, $a_8$ influence observables and are thereby tightly constrained; and, within the space we have searched, only $a_1$ has a material impact on the $k^2$-dependence of the mass function, illustrated in Fig. 5, left panel.

Further highlighting a plausible connection between the action of $a_1$ and a zero in the proton's electric form factor, $G_{Ep}$, Fig. 5, left panel, also depicts a comparison between the impact of $a_1$ on the $k^2$-dependence of the mass-function and that *assumed* for the effect of DCSB and vertex feedback in Ref. [56]: the similarity between the curves supports the conclusions drawn therein.

It is also worth remarking that the size of $M^0$ is largely determined by $a_{4\hat{5}}$: given a value of $a_{4\hat{5}}$, $a_{1,3,8}$ can vary within material subdomains of their search spaces without much affecting $M^0$. For instance, a value of $M^0 = 0.275$ GeV is maintained to within 0.2% when $a_{4\hat{5}} \in [-1.16, -0.68]$ (4%) and $a_1 \in [-0.6, 1.0]$ (80%), $a_3 \in [-1, 1]$ (100%), $a_8 \in [-3.4, 0.3]$ (60%), where the percentages indicate the size of the subdomain relative to that specified for the coefficient in Eq. (9).

The behaviour of the quark wave function renormalisation, $Z(p^2) = 1/A(p^2)$, is commonly overlooked in studies of DCSB and the gluon-quark vertex, possibly because its effects are often (implicitly) absorbed into the model interaction. This can lead, however, to results for $Z(p^2)$

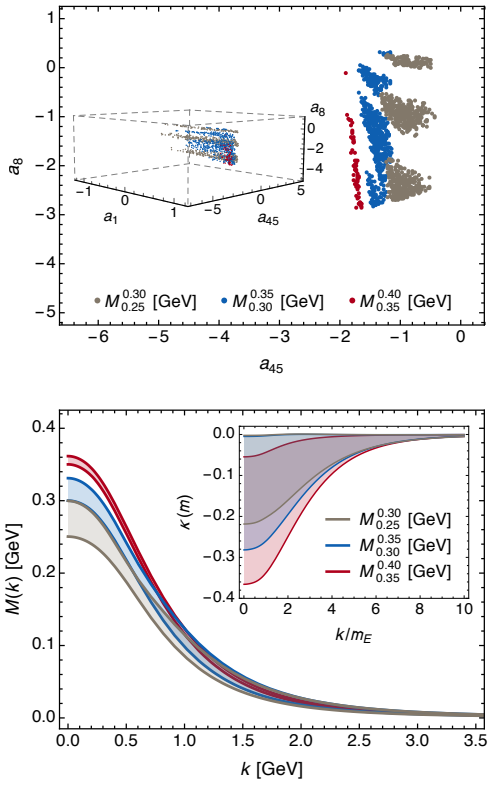


FIG. 3. Case C. *Upper panel* – Set of $(a_1, 0, a_{\hat{45}}, a_8)$ satisfying cuts $(i)$–$(iii)$. Inset shows 3D volume that survives all cuts and correlations between coefficients. Bands: light (grey), $M^0 \in (0.25, 0.30)$ GeV; dark (blue), $M^0 \in (0.30, 0.35)$ GeV; darker (red), $M^0 \in (0.35, 0.40)$ GeV. Few acceptable vertices lie in the last category. *Lower panel* – Associated mass functions (like-shaded bands) and ACMs (inset).

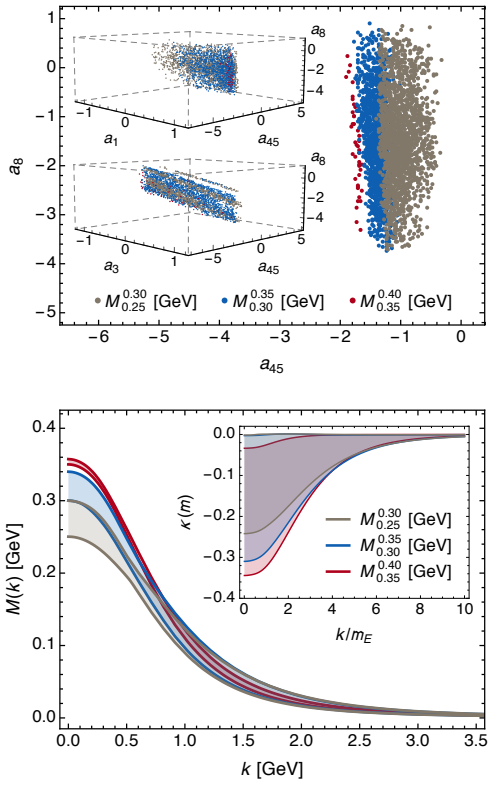


FIG. 4. Case D. *Upper panel* – Domain of coefficients satisfying cuts $(i)$–$(iii)$. The space is four-dimensional and the insets help display the hyper-volume that survives all cuts and the correlations between the coefficients. *Lower panel* – Mass functions produced by the vertices identified in the upper panel lie within the like-shaded bands. (Legend in Fig. 3.)

that conflict with known constraints, *e.g.* pQCD requires that in Landau gauge $Z(p^2) \to 1^-$ as $p^2 \to \zeta^{2-}$ [57]. This feature is preserved by all *Ansätze* that survive the cuts we apply. It is not sufficient, however, to ensure $Z(p^2)$ is monotonic on $p^2 \in [0, \zeta^2]$. That outcome is only guaranteed if one also requires $M^0 \gtrsim 0.35\,\text{GeV}$.

Fig. 5, right panel, depicts both the combined results from Cases A–D, with neighbourhoods of similar vertex coefficients sampled in all cases indicated by the domains of highest intensity, and highlights the interplay between the filtering criteria and $a_{1,3}$. Plainly, the criteria do not tightly constrain $a_3$, although, as remarked earlier, its presence does permit a larger domain of $a_8$ values in acceptable *Ansätze*. In connection with $a_1$, on the other hand, the allowed range of values depends on the magnitude of $M^0$: $-0.5 \lesssim a_1 \lesssim 1$ for $M^0 \in (0.26, 0.36)$ GeV.

Now, denoting by $\mathbb{G}_4$ that subdomain of considered vertices whose members each yield a gap equation solution consistent with criteria $(i)$–$(iii)$, then

$$\mathbb{G}_4 \subset \{(a_1, a_3, a_{\hat{45}}, a_8)\,|\,a_1 \in [-0.5, 1], a_3 \in [-1, 1], \\ a_{\hat{45}} \in [-2, -0.4]\,, a_8 \in [-4, 1]\} \subset \mathbb{V}_4\,. \quad (11)$$

It is obvious but nevertheless worth highlighting that the bare vertex, $\Gamma^{a0}_\mu$, is not a member of $\mathbb{G}_4$. In fact, using the RGI running-interaction explained in the Introduction, which unifies the top-down and bottom-up approaches to charting QCD's gauge sector, the bare vertex is incapable of inducing DCSB. Positive feedback, generated by, *e.g.* the $t_\nu \Delta^{qk}_B$ and $T_{4,5}$ terms in $\Gamma^a_\mu$, is necessary to achieve DCSB with a realistic interaction. Plainly, therefore, in order to secure a successful description of some subset of hadron observables with the widely-used rainbow-ladder DSE truncation [5, 25, 27, 58], the gap equation's kernel must include an unrealistic magnification at infrared-momenta. Hence, one should be cautious when developing an interpretation of results obtained in this way, *e.g.* those related directly to the pointwise behaviour of bound-state Bethe-Salpeter amplitudes will, at most, only be semi-quantitatively reliable [4, 59–62], and that will also impact upon level-ordering and -spacing in the hadron spectrum [6, 7, 31, 40, 63–69].

**4. Epilogue**. Using a renormalisation-group-invariant (RGI) running-interaction that joins top-down and bottom-up analyses of the gauge sector in quantum chromodynamics (QCD), we computed quark gap equation

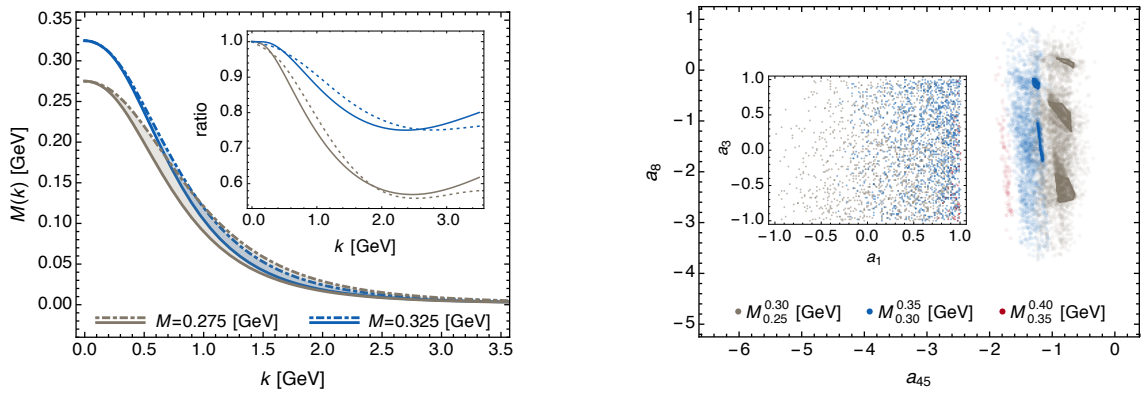


FIG. 5. *Left panel.* Impact of $a_1$ on $M(k)$. For fixed $M^0$, a larger $a_1$ value yields a mass-function that runs more rapidly with $k$ ($M_f(k)$, solid curves) than does a smaller $a_1$ value ($M_s(k)$, dot-dashed curves). *Inset*: Comparison of this effect, via the ratio $= M_f(k)/M_s(k)$, with that assumed in Ref. [56] – solid light (grey) curves depict ratio computed from the like curves in the main figure, dashed light curve is ratio obtained in Ref. [56] using $\alpha = 2$, the largest suppression of DCSB considered therein. ($\alpha = 1$ means no suppression.); solid dark (blue) curves, obtained from like curves in the main figure, and dark dashed curve, $\alpha = 1.4$ ratio in Ref. [56]. *Right panel.* Combined domains of vertex coefficients from Figs. 1–4. Highest intensity regions: neighbourhoods of similar coefficient values explored in all four cases; and lowest intensity regions, domains reached only in Case D. *Inset* – Distribution of allowed vertices in the $(a_1, a_3)$ plane. Evidently, criteria $(i)$–$(iii)$ place little constraint on $a_3$, whereas $a_1$ has a strong influence on the feedback necessary for DCSB, as illustrated in the left panel. Legend as in Figs. 3, 4.

solutions with 1.66-million distinct *Ansätze* for the gluon-quark vertex, $\Gamma_\mu$. The *Ansätze* were selected from a class whose members can uniquely be identified by a vector in $\mathbb{R}^4$, and those studied were selected at random from a compact subdomain, $\mathbb{V}_4$, whose limits were deliberately chosen to ensure consistency with extant explorations of the gauge-boson–fermion three-point function.

Each member of the set of gap equation solutions thus obtained was tested for compatibility with three criteria: $(i)$ does it express a physically reasonable amount of dynamical chiral symmetry breaking (DCSB); $(ii)$ is the associated quark anomalous chromomagnetic moment negative-definite; and $(iii)$ does it produce a value for the pion's leptonic decay constant that lies within 5% of its chiral-limit value? Remarkably, merely 0.55% of the solutions survived the test. Evidently, even a small selection of observables places very tight constraints on the domain of realistic vertex *Ansätze*, $\mathbb{G}_4$, so that $\mu(\mathbb{G}_4) \approx 0$ within $\mathbb{R}^4$, *i.e.* the hyper-volume occupied by the space of physically acceptable vertices is extremely small.

Of course, the Standard Model has a unique RGI running-interaction and a unique $\Gamma_\mu$; but so long as it is necessary for studies of hadron properties to make assumptions about the gluon-quark vertex, then our results will help ensure those assumptions are realistic.

**Acknowledgments**. DB acknowledges correspondence with H. Sanchis-Alepuz and D. Gazda. Our results were obtained using the KORE HPC of the Fondazione Bruno Kessler. Research supported by: Spanish MEYC under grants FPA2014-53631-C2-1-P and SEV-2014-0398, and Generalitat Valenciana under grant Prometeo II/2014/066; Argonne National Laboratory, Office of the Director, through the Named Postdoctoral Fellowship Program; and U.S. Department of Energy, Office of Science, Office of Nuclear Physics, contract no. DE-AC02-06CH11357.

**Appendix**. Here we list the tensors used in Eq (7b):

$$T^1_\nu = \tfrac{i}{2} t^{\rm T}_\nu \,,\; T^3_\nu = \gamma^{\rm T}_\nu \,,\; T^4_\nu = -i T^1_\nu \sigma_{\alpha\beta} q_\alpha k_\beta \,, \qquad (12)$$
$$T^5_\nu = \sigma_{\nu\rho} p_\rho \,,\; T^8_\nu = q_\nu \gamma\cdot k - k_\nu \gamma\cdot q + i\gamma_\nu \sigma_{\alpha\beta} q_\alpha k_\beta \,,$$

where $t^{\rm T}_\mu = T_{\mu\nu} t_\nu$, etc. To ease comparisons with Ref. [33], we remark that the vertex arguments must be mapped as follows: $q \to p_f$, $p_i \to k$ and $k \to p$, $t \to 2\ell$. Then, denoting the Dirac-tensor basis used therein for the transverse vertex as $\{\hat{T}^i_\nu, i = 1, \ldots, 8\}$: $\hat{T}^2_\nu = T^5_\nu$, $\hat{T}^3_\nu = T^3_\nu$, $\hat{T}^4_\nu = -T^8_\nu$, $\hat{T}^5_\nu = -T^1_\nu$, $\hat{T}^7_\nu = -2T^2_\nu$, $\hat{T}^8_\nu = -2T^4_\nu$, with $\hat{T}^{3,6}_\nu$ given by linear combinations of $T^{6,7}_\nu$, which are not needed herein. Consequently, the coefficient functions in Ref. [33] are identified with ours thus: $\hat{F}_1 = \tau_3$, $\hat{F}_2 = \tau_5$, $\hat{F}_4 = -\tau_8$, $\hat{F}_5 = -\tau_1$ $\hat{F}_7 = -\frac{1}{2}\tau_2$, $\hat{F}_8 = -\frac{1}{2}\tau_4$.

[1] Y. Nambu and G. Jona-Lasinio, Phys. Rev. **122**, 345 (1961).
[2] K. D. Lane, Phys. Rev. D **10**, 2605 (1974).
[3] H. D. Politzer, Nucl. Phys. B **117**, 397 (1976).
[4] L. Chang *et al.*, Phys. Rev. Lett. **110**, 132001 (2013).
[5] P. Maris and C. D. Roberts, Phys. Rev. C **56**, 3369 (1997).
[6] S.-X. Qin, L. Chang, Y.-X. Liu, C. D. Roberts and D. J. Wilson, Phys. Rev. C **84**, 042202(R) (2011).
[7] S.-X. Qin, L. Chang, Y.-X. Liu, C. D. Roberts and D. J.

Wilson, Phys. Rev. C **85**, 035202 (2012).
[8] P. Jain and H. J. Munczek, Phys. Rev. D **48**, 5403 (1993).
[9] J. C. R. Bloch, Phys. Rev. **D66**, 034032 (2002).
[10] A. Aguilar, D. Binosi and J. Papavassiliou, Phys. Rev. D **78**, 025010 (2008).
[11] P. Boucaud *et al.*, Few Body Syst. **53**, 387 (2012).
[12] A. C. Aguilar, D. Binosi and J. Papavassiliou, Front. Phys. China **11**, 111203 (2016).
[13] D. Binosi, L. Chang, J. Papavassiliou and C. D. Roberts, Phys. Lett. B **742**, 183 (2015).
[14] J. M. Cornwall, Phys. Rev. D **26**, 1453 (1982).
[15] J. M. Cornwall and J. Papavassiliou, Phys. Rev. D **40**, 3474 (1989).
[16] D. Binosi and J. Papavassiliou, Phys. Rev. D **66**, 025024 (2002).
[17] D. Binosi and J. Papavassiliou, Phys. Rept. **479**, 1 (2009).
[18] A. Aguilar, D. Binosi, J. Papavassiliou and J. Rodríguez-Quintero, Phys. Rev. D **80**, 085018 (2009).
[19] J. S. Ball and T.-W. Chiu, Phys. Rev. D **22**, 2542 (1980).
[20] A. G. Williams, G. Krein and C. D. Roberts, Annals Phys. **210**, 464 (1991).
[21] D. C. Curtis and M. R. Pennington, Phys. Rev. D **42**, 4165 (1990).
[22] C. J. Burden and C. D. Roberts, Phys. Rev. D **44**, 540 (1991).
[23] Z.-H. Dong, H. J. Munczek and C. D. Roberts, Phys. Lett. **B333**, 536 (1994).
[24] A. Bashir and M. Pennington, Phys. Rev. D **50**, 7679 (1994).
[25] H. J. Munczek, Phys. Rev. D **52**, 4736 (1995).
[26] M. Stingl, Z. Phys. A **353**, 423 (1996).
[27] A. Bender, C. D. Roberts and L. von Smekal, Phys. Lett. B **380**, 7 (1996).
[28] F. T. Hawes, P. Maris and C. D. Roberts, Phys. Lett. B **440**, 353 (1998).
[29] M. S. Bhagwat, A. Höll, A. Krassnigg, C. D. Roberts and P. C. Tandy, Phys. Rev. C **70**, 035205 (2004).
[30] M. S. Bhagwat and P. C. Tandy, Phys. Rev. D **70**, 094039 (2004).
[31] L. Chang and C. D. Roberts, Phys. Rev. Lett. **103**, 081601 (2009).
[32] A. Kızılersü and M. R. Pennington, Phys. Rev. D **79**, 125020 (2009).
[33] L. Chang, Y.-X. Liu and C. D. Roberts, Phys. Rev. Lett. **106**, 072001 (2011).
[34] A. C. Aguilar and J. Papavassiliou, Phys. Rev. D **83**, 014013 (2011).
[35] S.-X. Qin, L. Chang, Y.-X. Liu, C. D. Roberts and S. M. Schmidt, Phys. Lett. B **722**, 384 (2013).
[36] A. C. Aguilar, D. Binosi, D. Ibañez and J. Papavassiliou, Phys. Rev. D **90**, 065027 (2014).
[37] A. Kızılersü, T. Sizer, M. R. Pennington, A. G. Williams and R. Williams, Phys. Rev. D **91**, 065015 (2015).
[38] M. Mitter, J. M. Pawlowski and N. Strodthoff, Phys. Rev. D **91**, 054035 (2015).
[39] D. Binosi, L. Chang, J. Papavassiliou, S.-X. Qin and C. D. Roberts, Phys. Rev. D **93**, 096010 (2016).
[40] L. Chang and C. D. Roberts, Phys. Rev. C **85**, 052201(R) (2012).
[41] H. Sanchis-Alepuz and R. Williams, Phys. Lett. B **749**, 592 (2015).
[42] S.-X. Qin, EPJ Web Conf. **113**, 05024 (2016).
[43] Y. Takahashi, (1985), *Canonical quantization and generalized Ward relations: Foundation of nonperturbative approach*, Print-85-0421 (Alberta).
[44] H.-X. He, F. Khanna and Y. Takahashi, Phys. Lett. **B480**, 222 (2000).
[45] M. Pennington and R. Williams, J. Phys. G **32**, 2219 (2006).
[46] H.-X. He, Phys. Rev. D **80**, 016004 (2009).
[47] J. Skullerud and A. Kizilersu, JHEP **09**, 013 (2002).
[48] H.-W. Lin, Phys. Rev. D **73**, 094511 (2006).
[49] A. Kızılersü, D. B. Leinweber, J.-I. Skullerud and A. G. Williams, Eur. Phys. J. **50**, 871 (2007).
[50] E. Rojas, J. P. B. C. de Melo, B. El-Bennich, O. Oliveira and T. Frederico, JHEP **10**, 193 (2013).
[51] A. Bashir, R. Bermúdez, L. Chang and C. D. Roberts, Phys. Rev. C **85**, 045205 (2012).
[52] J. Gasser and H. Leutwyler, Annals Phys. **158**, 142 (1984).
[53] H. Pagels and S. Stokar, Phys. Rev. **D20**, 2947 (1979).
[54] R. T. Cahill and C. D. Roberts, Phys. Rev. **D32**, 2419 (1985).
[55] P. Maris, C. D. Roberts and P. C. Tandy, Phys. Lett. B **420**, 267 (1998).
[56] I. C. Cloët, C. D. Roberts and A. W. Thomas, Phys. Rev. Lett. **111**, 101803 (2013).
[57] A. I. Davydychev, P. Osland and L. Saks, Phys. Rev. D **63**, 014022 (2001).
[58] P. Maris and P. C. Tandy, Phys. Rev. C **60**, 055214 (1999).
[59] T. Nguyen, N. A. Souchlas and P. C. Tandy, AIP Conf. Proc. **1361**, 142 (2011).
[60] I. C. Cloët, L. Chang, C. D. Roberts, S. M. Schmidt and P. C. Tandy, Phys. Rev. Lett. **111**, 092001 (2013).
[61] M. Ding, F. Gao, L. Chang, Y.-X. Liu and C. D. Roberts, Phys. Lett. B **753**, 330 (2016).
[62] T. Horn and C. D. Roberts, J. Phys. G. **43**, 073001/1 (2016).
[63] A. Krassnigg, Phys. Rev. D **80**, 114010 (2009).
[64] A. Krassnigg and M. Blank, Phys. Rev. D **83**, 096006 (2011).
[65] H. L. L. Roberts, L. Chang, I. C. Cloët and C. D. Roberts, Few Body Syst. **51**, 1 (2011).
[66] C. Chen, L. Chang, C. D. Roberts, S.-L. Wan and D. J. Wilson, Few Body Syst. **53**, 293 (2012).
[67] E. Rojas, B. El-Bennich and J. P. B. C. de Melo, Phys. Rev. D **90**, 074025 (2014).
[68] M. Gómez-Rocha, T. Hilger and A. Krassnigg, Phys. Rev. D **92**, 054030 (2015).
[69] G. Eichmann, H. Sanchis-Alepuz, R. Williams, R. Alkofer and C. S. Fischer, Prog. Part. Nucl. Phys. **91**, 1 (2016).